Available online at www.sciencedirect.com
SCIENCE DIRECT
Catalysis Today 107–108 (2005) 139–148
CATALYSIS TODAY
www.elsevier.com/locate/cattod

Catalytic abatement of NO_x: Chemical and mechanistic aspects

Guido Busca *, Maria Angeles Larrubia [1], Laura Arrighi, Gianguido Ramis

Laboratorio di Chimica delle Superfici e Catalisi Industriale, Dipartimento di Ingegneria Chimica e di Processo, Università di Genova, P.le J.F. Kennedy, 16129 Genova, Italy

Available online 24 August 2005

Abstract

The chemical and mechanistic aspects of the selective catalytic reduction (SCR) of NO by ammonia and by methane have been investigated. In the classical NH_3-SCR process, operating near 600 K over vanadia-titania based catalysts, ammonia is activated by coordination over Lewis acid sites and reacts with gas phase or weakly adsorbed NO. The same mechanism occurs for the low-temperature (400–500 K) NH_3-SCR over Mn and Fe based catalysts. On the contrary, low-temperature NH_3-SCR over protonic zeolites implies the activation of ammonia as ammonium ions and the previous oxidation of part of NO to NO_2. The CH_4-SCR over Co-zeolite catalysts is supposed to imply the activation of NO_x in the form of an adsorbed oxidized species, that reacts with the reductant, CH_4, from the gas phase or activated by adsorption into the zeolite channels. The other catalytic denoxing technologies, like the NO decomposition over Cu-zeolite based catalysts, the N_2O decomposition over noble or transition metal based catalysts, the storage-reduction on Ba-aluminate based catalysts and the reduction by CO over noble metal based three way catalysts, imply a strong adsorption and activation of NO_x over the surface, although activation of hydrocarbons and CO over the noble metals can also be helpful in the last two cases.

Keywords: deNO$_x$; NO$_x$ abatment; Mechanism of denoxing; Selective catalytic reduction

1. Introduction

Mixtures of NO, NO_2 and N_2O produced by combustion engines and industrial processes contribute to different atmospheric pollution phenomena. Although several other nitrogen oxides exist, NO_x generally refers to a mixture of NO and NO_2, to which N_2O must be added, which are the stable species in the gas phase at room or higher temperature and low partial pressures. While NO is non-toxic by itself at low concentrations and has a very relevant biochemical role when formed in the human body [1], it contributes to ozone formation. Nitrogen dioxide (NO_2) is a reddish brown, highly reactive and more toxic gas. Once it has formed, nitrogen dioxide can react with other pollutants (volatile organic compounds). NO and NO_2 are involved in the photochemical smog and acid rains phemomena. Their emissions are regulated by law. N_2O is a non-toxic substance (at low concentration levels) and is still not regulated. However, it is a well-known ''greenhouse'' gas and also is involved in stratospheric ozone destruction, so it is expected it will be limited shortly.

In recent years, great efforts have been applied to the widespread application of available technologies to limit emission of such air pollutants [2]. In particular, different catalytic abatement technologies, either applied to mobile sources [3] or to stationary sources [4], have been developed starting from the eighties, and new processes are nowadays under study to fulfill new stricter limits. Some chemical and mechanistic aspects of such catalytic processes have been newly investigated. Here, the results of this study are summarized and comparisons between technologies are made.

2. Experimental

Thermodynamic calculation has been based on the data reported by Reid et al. [5]. The surface reaction mechanisms

* Corresponding author.
E-mail address: Guido.Busca@unige.it (G. Busca).
[1] On leave from Departamento de Ingenieria Quimica, Universidad de Malaga, Spain

0920-5861/$ – see front matter © 2005 Elsevier B.V. All rights reserved.
doi:10.1016/j.cattod.2005.07.077

were mainly investigated using infrared technique. IR spectra were recorded on a Nicolet Protégé 460 Fourier Transform instruments. The adsorption experiments have been performed using pressed disks of pure powders (15 mg for 2 cm diameter), activated by outgassing at 773 K into the IR cell. A conventional manipulation/outgassing ramp connected to the IR cell was used. The adsorption procedure involves contact of the activated samples disk with vapours at RT, at a pressure of 1–15 Torr and outgassing in steps at RT and increasing temperatures.

3. Results and discussion

3.1. Thermodynamics of NO_x formation, decomposition and reduction

The reaction of NO formation from air's N_2 and O_2 (''thermal NO_x''):

$$N_2 + O_2 \leftrightarrows 2NO \quad \Delta H^\circ_{298} = 180.6\,\text{kJ} \tag{1}$$

is very unfavored from the thermodynamic point of view, but allows the production of some hundreds of ppmv of NO at temperatures of 1300 K up to few thousands ppmv at higher temperatures (Fig. 1). Notably, the reaction can be catalyzed by materials in contact with the flame, some of which acting as promoters of NO, others being instead inhibitors. This is obviously relevant in particular for fluidised bed solid combustors [6]. The amount of thermal NO_x after combustion, consequently, depends on the reaction peak temperature in the combustors, and consequently on the design of the combustor itself. Low-NO_x burners, where combustion peak temperatures are smoothed by partial premixing, are today available [7].

On the contrary, the oxidation of nitrogen containing compounds, such as ammonia and amines, to NO:

$$2NH_3 + \tfrac{5}{2}O_2 \rightarrow 2NO + 3H_2O \quad \Delta H^\circ_{298} = -452\,\text{kJ} \tag{2}$$

is fully favored thermodynamically, although less favored than the oxidation to nitrogen. So, the amount of ''fuel NO_x'' primarily depends from the amount of nitrogen in the fuel, although it is also strongly influenced by reactor design. Nitrogen compounds are virtually absent when methane is the fuel. However, substantial amounts of fuel nitrogen exist in the cases of the use of coal, gasoils and fuel oils as well as biomasses, such as wood, as fuels. In these cases, the amount of ''fuel NO_x'' may be relevant, although usually it does not exceed few hundreds of ppmv. To limit the production of fuel NO_x in the presence of fuel nitrogen, quite complex combustion plant must be built up, with a first ''reduction furnace'' operating near 1370 K in defect air, allowing all nitrogen to be converted to N_2, a quenching by recycled stack gas down to 1000–1100 K and a further oxidation step to convert most carbon species to CO_2 in excess air near 1200 K [8].

A third more complex mechanism produces NO, involving the reaction of molecular nitrogen with organic radicals with the intermediacy of HCN (''prompt NO_x''). This mechanism occurs at temperatures of 1500 K or above and may give rise to several tens of ppm of NO. The back reaction of NO decomposition to give N_2 and O_2 is extremely slow and practically it does not occur, so that once formed NO does not decompose spontaneously.

At lower temperature NO can further react with oxygen to give NO_2:

$$NO + \tfrac{1}{2}O_2 \leftrightarrows NO_2 \quad \Delta H^\circ_{298} = -113\,\text{kJ/mol} \tag{3}$$

This reaction is fully shifted to (the) left at high temperature, thus NO is the product formed upon combustion. However, the equilibrium fully shifts to (the) right in air and also in oxygen-depleted air at temperatures near 500 K or below (Fig. 2). So, NO could be fully converted to NO_2 in principle. However, this reaction too is very slow at concentrations as low as few hundreds of ppm. As a result of this, the NO_x mixture in air is usually still mostly composed of NO.

At low-temperature NO can also be converted to N_2O:

$$2NO \leftrightarrows N_2O + \tfrac{1}{2}O_2 \quad \Delta H^\circ_{298} = -99\,\text{kJ} \tag{4}$$

This reaction is favored at low-temperature (Fig. 3) but is unfavored at high temperature. For this reason N_2O can also

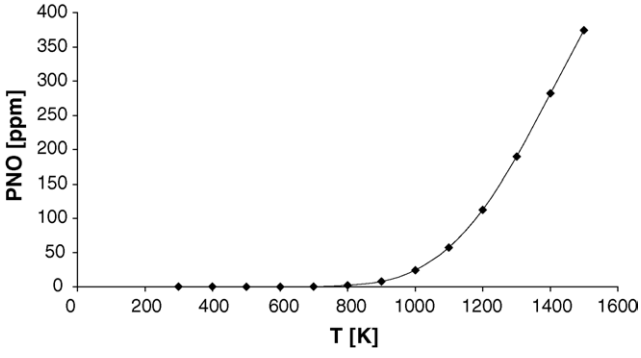

Fig. 1. Theoretical equilibrium NO concentration in air.

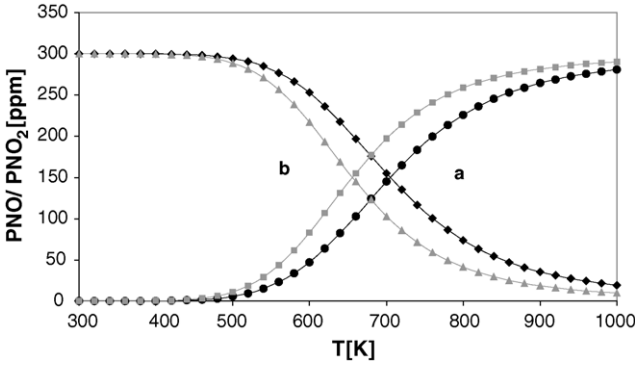

Fig. 2. Theoretical equilibrium concentration of NO (●, ■) and NO_2 (◆, ▲) starting from NO + NO_2 = 300 ppm in air (●, ◆) and in oxygen depleted air (■, ▲).

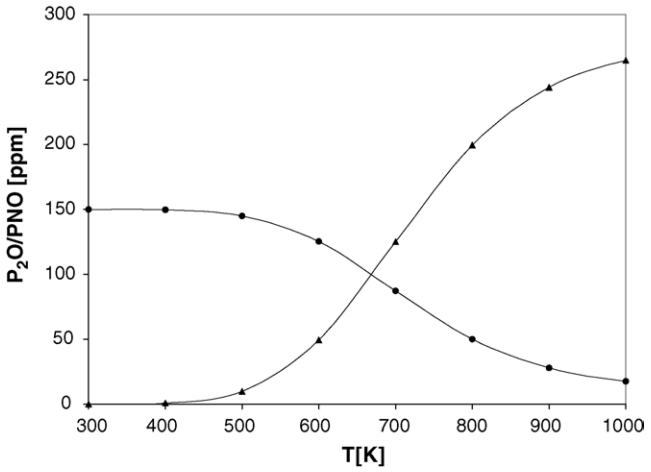

Fig. 3. Theoretical equilibrium concentration of NO (▲) and N_2O (●) (starting from N_2O 150 ppm) in air.

be intermediate in the formation of NO upon combustion at high temperature. On the other hand, for the same reason, N_2O can also be (but not necessarily is) intermediate in the reduction of NO to N_2 at low-temperature.

At high pressure and low-temperatures, NO is also instable with respect to its disproportionation:

$$3NO \leftrightarrows N_2O + NO_2 \quad \Delta H^\circ_{298} = -155\,kJ \tag{5}$$

This reaction is very slow, if any, at NO partial pressures of hundreds of ppm, but is fast at pressures of some atmospheres, so that it can cause contamination of NO gas by N_2O and NO_2 in high pressure NO cylinders. For this reason purification of NO is usually needed and sometimes is not prefect.

As said, N_2O is more stable than NO at low-temperature. However, reactions allowing the formation of N_2O, such as

$$4NH_3 + 4O_2 \rightarrow 2N_2O + 6H_2O \quad \Delta H^\circ_{298} = -1103\,kJ \tag{6}$$

$$4NH_3 + 4NO + 3O_2 \rightarrow 4N_2O + 6H_2O \tag{7}$$

are thermodynamically favored also at high temperatures. So, the formation of significant amounts of N_2O upon oxidation processes is possible. However, the main sources of N_2O are chemical processes, like nitric acid synthesis by ammonia oxidation and adipic acid synthesis by cyclohexanone oxidation in nitric acid:

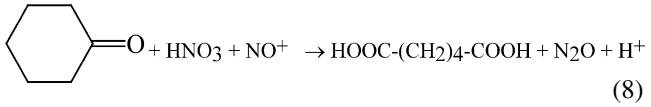

(8)

as well as the conversion of fertilizers in soils.

The equilibrium dimerization of NO:

$$2NO \leftrightarrows N_2O_2 \quad \Delta H^\circ_{298} < 0 \tag{9}$$

is likely an intermediate step in reactions (3)–(5), and this explains some unusual kinetic features. This reaction is also relevant in the liquid phase [9]. However, the existence of N_2O_2 as well as of other nitrogen oxides such as NO_3, N_2O_3, N_2O_4 and N_2O_5 [10] in the gas phase may be neglected in the context of the present work.

The decomposition of NO, i.e. the reverse of reaction (1′),

$$NO \leftrightarrows \tfrac{1}{2}N_2 + \tfrac{1}{2}O_2 \quad \Delta H^\circ_{298} = -90.3\,kJ/mol \tag{1′}$$

is thermodynamically strongly favored, but it does not occur spontaneously for kinetic reasons. Although several materials can catalyze it, not enough active and resistant catalysts have been found yet; extensive research is still active in this field [11].

The selective reduction of NO to nitrogen can be efficiently accomplished in principle by using different reductants.

$$NO + CO \rightarrow \tfrac{1}{2}N_2 + CO_2 \quad \Delta H^\circ_{298} = -328\,kJ/mol \tag{10}$$

$$4NO + 4NH_3 + O_2 \rightarrow 4N_2 + 6H_2O \quad \Delta H^\circ_{298} = -1627\,kJ/mol \tag{11}$$

$$NO + CH_4 + \tfrac{3}{2}O_2 \rightarrow \tfrac{1}{2}N_2 + CO_2 + 2\,H_2O \quad \Delta H^\circ_{298} = -847\,kJ/mol \tag{12}$$

$$NO + H_2 \rightarrow \tfrac{1}{2}N_2 + H_2O \quad \Delta H^\circ_{298} = -287\,kJ/mol \tag{13}$$

Also these reactions, however, need of catalysts to be performed selectively, without formation of N_2O, at sufficiently low-temperature. CO (reaction (10)) is the actual reductant in the so-called ‘‘three way’’ catalysts used for gasoline engines working in reducing conditions and ammonia is used as the reductant in the so-called SCR process largely applied to stationary sources in oxygen excess. The use of methane as the reductant could be a good choice alternative to ammonia in several industrial plants working in excess oxygen, but is still not commercialized. The use of hydrogen seems less attractive today and not practical in oxidizing conditions.

As said, the decomposition of N_2O

$$N_2O \leftrightarrows N_2 + \tfrac{1}{2}O_2 \quad \Delta H^\circ_{298} = -82\,kJ/mol \tag{14}$$

is also thermodynamically favored, but it does not occur spontaneously for kinetic reasons. It may be quite efficiently catalyzed although at very high temperatures, over transition metal oxides and by noble metals [12,13]. Industrial processes are already applied, e.g. for purification of waste gases from adipic acid plants. Consequently, the use of reductants to convert N_2O into nitrogen does not seem to be an attractive solution.

The data reported above, among other things, show that N_2O can be (but not necessarily is) intermediate both in NO formation at high temperature and in NO reduction at low-temperature. On the other hand, they also show that in oxidizing atmosphere NO_2 may be present in substantial amounts together with NO, so that it could in principle act as an intermediate in the reduction reactions.

3.2. The NH_3-SCR process

3.2.1. NH_3-SCR over V_2O_5-WO_3 (MoO_3)/TiO_2 catalysts

DeNOxing of waste gases from stationary sources can be achieved efficiently by using the so-called selective catalytic reduction process (SCR). For instance, about 80% of the current industrial DeNOxing is carried out by this technology. In this case, ammonia injected in the waste gases is used as the reducing agent. This technology has been first developed in Japan in the seventies, but many chemical aspects of this technology are still object of discussion in the scientific literature.

Industrial catalysts are constituted by V_2O_5-WO_3/TiO_2 or V_2O_5-MoO_3/TiO_2 catalysts, constituted by TiO_2 anatase supports at whose surface a ''monolayer'' of V_2O_5 and WO_3 (or MoO_3) have been deposited by impregnation. In general, the overall surface area of the catalysts is 50–100 m^2/g, with V_2O_5 virtual contents of 0.5–3% (w/w) and MoO_3 or WO_3 contents of 5–10% (w/w).

Infrared and Raman studies show that vanadyl, wolframyl and molybdenyl species are present on the dry surfaces of these catalysts. All these species are characterized by single bands at the same position in IR and Raman spectra, as well as by single overtone bands well detectable in the IR spectra (Table 1). As discussed elsewhere, the absence of any splitting in both fundamental and overtone region is a strong evidence for an isolated monoxo structure for these species. In fact, both dioxo species and polymeric monoxo species [14] give rise to split bands because of the coupling of the different M=O stretching modes. In this case, additionally, the strongest IR active band should not coincide with the strongest Raman band, so that the bands (even if not clearly split) should not have the same position in IR and Raman. On the other hand, it is also possible that small amounts of polymeric species may be present, in particular for wolframate and molybdate species whose coverage is generally high (8–12%, w/w).

In the above table are also reported the position of additional bands which are also present in industrial $DeNO_x$ catalysts and that provide evidence for sulphate species, which are also in the form of monooxo orthosulphates, and of silica or glass particles which are added to improve the mechanical properties of the catalyst [15].

In Fig. 4, the infrared spectrum of a commercial V_2O_5-MoO_3/TiO_2 (V_2O_5 1.2%, w/w; MoO_3 6.2%, w/w) spent catalyst as recovered from metal plate monolyths after use for several months is reported. The presence of glass particles obscures most of the fundamental stretching region below 1250 cm^{-1}. However, the sharp weak band at 1978 cm^{-1} and a very weak shoulder near 2040 cm^{-1} are indicative of the presence, after outgassing, of free monooxo molybdenyl and vanadyl species, respectively. The strong maximum at 1375 cm^{-1} is due to S=O stretching of surface sulphate species, which are also responsible for overtone absorptions in the region 2300–2000 cm^{-1}. Absorptions near 2000, 1850 and 1620 cm^{-1} are overtone bands of silica-based materials. No spectroscopic features are observed due to adsorbed species. The spectrum is almost identical to that of the corresponding fresh catalyst showing that no irreversible deposition of molecules occurred upon time on stream. After adsorption of ammonia, the bands of surface vanadyl, molybdenyl and sulphate species are perturbed, and strong bands due to adsorbed ammonia species are formed. The strong band at 1435 cm^{-1} and the broad strong absorption in the region 3100–2700 cm^{-1} are certainly due to ammonium cations, showing the presence of Brønsted acid sites on the surface. The absorption in the region 3400–3100 cm^{-1} and most of the strong band near 1600 cm^{-1} are instead associated to ammonia coordinatively bound over Lewis acid sites.

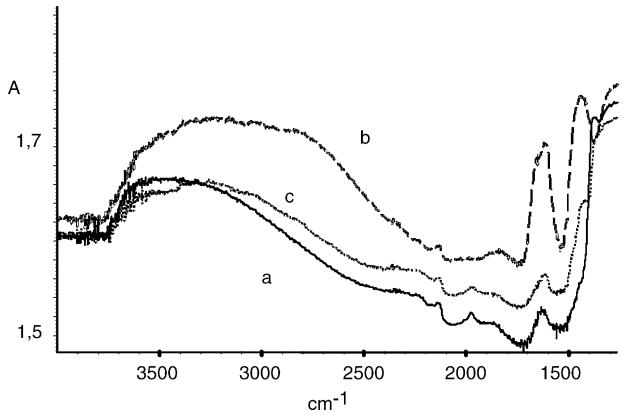

Fig. 4. FT-IR spectra of a spent commercial V_2O_5-MoO_3/TiO_2 catalyst after outgassing at 623 K (a), after contact with ammonia gas and outgassing at RT (b) and at 523 K (c).

In Fig. 5A, the IR spectra of ammonia adsorbed over a model V_2O_5-MoO_3/TiO_2 (V_2O_5 1%, w/w; MoO_3 10%, w/w) catalyst are reported. The spectra show the presence of two types of adsorbed species. The broad absorptions with maxima at 2990 and 2810 cm^{-1}, and the strong maximum at 1445 cm^{-1}, together with a weaker one at 1685 cm^{-1}, are characteristic of ammonium ions (asymmetric and symmetric NH_4 stretchings, symmetric and asymmetric NH_4 deformations, respectively). Instead, the NH streatchings in the region 3400–3150 cm^{-1}, and the asymmetric and symmetric deformations at 1605 and 1247 cm^{-1} are typically due to ammonia coordinated over Lewis acid sites. By outgassing at 423 K the bands due to ammonium ions decrease strongly in intensity while those due to

Table 1
Position of IR and Raman bands typically observed for commercial V_2O_5-WO_3/TiO_2 and V_2O_5-MoO_3/TiO_2 SCR catalysts

Mode	Stretching fundamentals (cm^{-1})	Stretching first overtones (cm^{-1})
V=O	1035	2040
W=O	1015	2014
Mo=O	1005	1978
S=O	1375	2300–2000
Si–O–Si(Al)	1250–1000	2000, 1850 and 1620

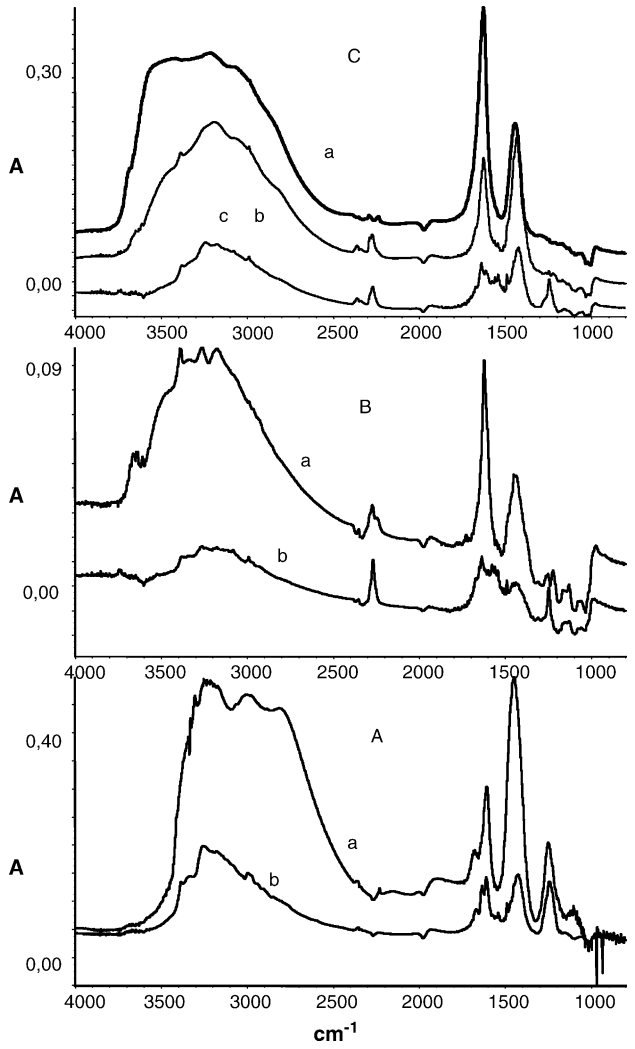

Fig. 5. FT-IR spectra of the adsorbed species (subtraction spectra) over a homemade model V_2O_5-MoO_3/TiO_2 catalyst after outgassing at 623 K and after contact with (A): ammonia gas and outgassing at RT (a) and at 423 K (b); (B): hydroxylamine vapour and outgassing at RT (a) and at 423 K (b); (C) hydrazine vapour at RT (a) and outgassing at RT (b) and at 423 K (c).

coordinated ammonia decrease much less and are now well evident at 3384, 3335, 3254, 3175, 1609 and 1241 cm^{-1}. Interestingly, a splitting is evident for the band near 1605 cm^{-1} with the appearance of a new component at 1633 cm^{-1}, while two sharp bands also appear at 1538 and 1488 cm^{-1}, which provide evidence for the formation of new species. These data show that ammonium ions, formed by ammonia protonation over Brønsted acid sites are much less stable than coordinated ammonia. Moreover, some ammonia transformation could also be occurred at 423 K. From the point of view of the chemistry, model and commercial catalysts behave closely.

In Fig. 5B, the spectra of the adsorbed forms arising from hydroxylamine adsorption on the same catalyst are reported. Here, two main maxima are found at 1620 and 1471 cm^{-1}. The former band can be assigned to the NH_2 bending of an adsorbed NH_2–O species. As reported for hydroxylamine adsorbed on Fe-TiO_2 catalysts, it seems likely that NH_2OH, which is a weak Brønsted acid, can dissociate on the surface and can form such anions. The band at 1475 cm^{-1}, very strong here, has been discussed and assigned previously to HNO species. By increasing outgassing temperature up to 423 K most bands decrease in intensity while a couple of sharp bands are now very evident at 2270 and 1241 cm^{-1}. They can be assigned to the asymmetric and symmetric stretching of adsorbed N_2O. It seems interesting to show here that while N_2HOH adsorbed on Fe-based catalysts easily produces NO here it mostly produces N_2O. On the other hand, HNO species are considered to be intermediates just in the formation of N_2O from hydrazine.

In Fig. 5C, the spectra of the adsorbed forms arising from hydrazine adsorption are also reported. A strong broad band is observed in the region 3600–3200 cm^{-1}, with the maximum at 3188 cm^{-1} and evident components at 3465 cm^{-1} (broad), 3190 cm^{-1} (sharp) and 3050 cm^{-1} (broad). Two strong bands are observed in the lower frequency region at 1625 and 1428 cm^{-1}. By outgassing, the broad band in the NH stretching region strongly decreases in intensity, while the band in the 1600 cm^{-1} region clearly splits to 1637 and 1608 cm^{-1}. Sharp bands appear at 1540 and 1488 cm^{-1}, together with the absorptions of N_2O observed here at 2270 and 1242 cm^{-1}. The band near 1428 cm^{-1}, which shifts to 1418 cm^{-1} by outgassing, does not correspond to NH bands below 3000 cm^{-1}, and this excludes their possible assignment to NH_4^+ ammoniun ions.

The data reported here, and in particular the similarity of some features concerning ammonia and hydrazine adsorption strongly suggest that ammonia can convert into hydrazine species. In particular, the band observed near 1635 cm^{-1} is likely due to hydrazine in both cases. A possible assignment for the band at 1540 cm^{-1} found also in both cases is to a NH_2 (amido) species while the band found at 1488 cm^{-1} from ammonia and hydrazine may correspond to the band found at 1475 cm^{-1} from hydrazine, and is likely due to nitroxyl species, which later transforms into N_2O. The strong band at 1418 cm^{-1} found from hydrazine, but possibly also from ammonia, could be due to NH (amido) species.

In Fig. 6, the subtraction spectra relative to the adsorption of ammonia over a MoO_3-TiO_2 catalyst (upper spectrum) and of further adsorption and reaction of NO over the ammonia covered sample, are reported. It is evident that the bands of coordinated ammonia (3390, 3345, 3262 and 3170 cm^{-1}, NH stretchings, 1602 cm^{-1} (NH_3 asymmetric deformation) and 1251 and 1206 cm^{-1} (NH_3 symmetric deformations, two different species) are present as negative bands, due just to the reaction of coordinated ammonia with NO. In contrast, the features of ammonium ions do not appear in the spectrum, just because they do not react, while the features of adsorbed water (OH stretchings at 3600–3500 cm^{-1}, H_2O bending at 1650 cm^{-1}), which is the IR detectable product of the SCR reaction are evident. Together bands at 2285 and 1801 cm^{-1}, due to adsorbed N_2O (a by-product) and NO are also evident.

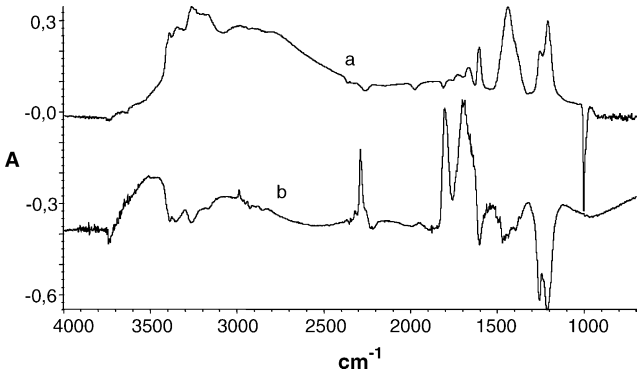

Fig. 6. FT-IR spectra of the adsorbed species (subtraction spectra) over a homemade model V_2O_5-MoO_3/TiO_2 catalyst: (a) after outgassing at 623 K, contact with ammonia gas and outgassing at RT; (b) subtraction spectrum after further contact with NO gas at 373 K: bands up species formed, bands down species disappeared.

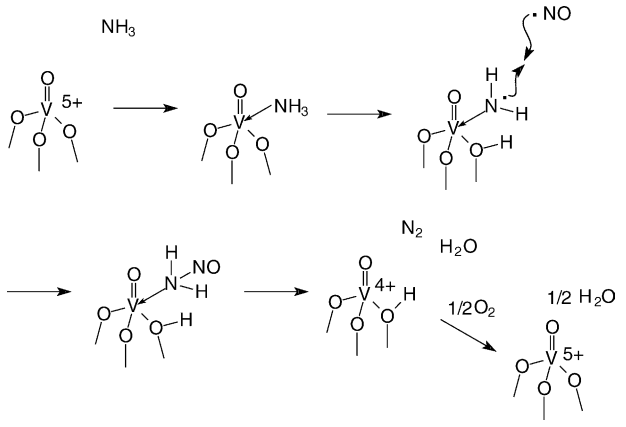

Scheme 1. A pathway for the NH_3-SCR process over vanadia-based catalysts.

These data agree with the chemical and mechanistic aspect of this process as they have been discussed in detail some years ago [16]. It is quite established that the reaction occurs between strongly adsorbed ammonia and gas phase or weakly adsorbed NO. Bosch and Janssen [17] demonstrated that the reaction is actually a coupling of NO with ammonia and that N_2O is not intermediate. However, disagreement exists on whether coordinated or protonated ammonia play(s) the role of reactive intermediate species. Since then, new relevant contribution appeared in the open literature, in particular concerning the reaction mechanism [18,19] and the role of preoxidation of NO to NO_2 [20]. Although disagreement still exists in the literature, most data seem to confirm, in the opinion of the present author, the role of vanadium (and also if molybdenum sites for Mo-TiO_2) cations as Lewis sites in adsorbing and activating ammonia, and the role of nitrosamide-like intermediates. Coordinated ammonia would be oxidized to amide species which later react(s) with NO giving adsorbed nitrosamide. This compound(s) decomposes into nitrogen and water while oxygen reoxidizes the catalyst surface. This mechanism, first proposed by Ramis et al. [21] has been successfully verified recently by computer modelling by Jug et al. [19]. IR spectra for V_2O_5-TiO_2 [21] as well as for V_2O_5-WO_3/TiO_2 [22] are similar to those presented here for MoO_3-TiO_2. They show very clearly that the coordinated ammonia disappears upon reaction with NO and water is formed. On the contrary, at least at the first stages of reaction, protonated ammonia grows more than disappear. NO is the actual reactant but the presence of NO_2 enhances the reaction rate, possibly because of its role in reoxidizing the catalyst (Scheme 1).

3.2.2. Low-temperature NH_3-SCR over transition metal oxide-based catalysts

The reduction of NO by ammonia should conveniently be performed at low-temperature (370–520 K) in tail-end process configuration, where the SCR reactor is placed after dust abatement and DESOXing steps. Here, the operating condition(s) are better for the catalyst but stack gas re-heating is unavoidable. Consequently, there is a great interest in developing active SCR catalysts that work at low-temperature, less than 520 K, but the limit of this potential technology consists in the total absence of SO_x in the gases, needed for it. In fact, at this temperature, the formation of ammonium sulphate with a consequent catalyst poisoning (and further other problems in the plant) occurs. Similarly (even in the absence of SO_x), ammonium nitrate can be formed and give several problems below 420 K.

Highly loaded V_2O_5-TiO_2, as well as Mn and Fe oxides supported on titania and alumina are active in the NH_3-SCR at low-temperature. In the temperature range 400–500 K, very high conversions of NO can be obtained in depending on the contact time. Mn- and Fe-containing catalysts may be even more active than V-based catalysts. However, selectivity to N_2 may be not total in these conditions, with significant production of N_2O.

In Fig. 7a and b, the spectra of ammonia adsorbed over a very active 7% MnO_x-TiO_2 catalyst are reported.

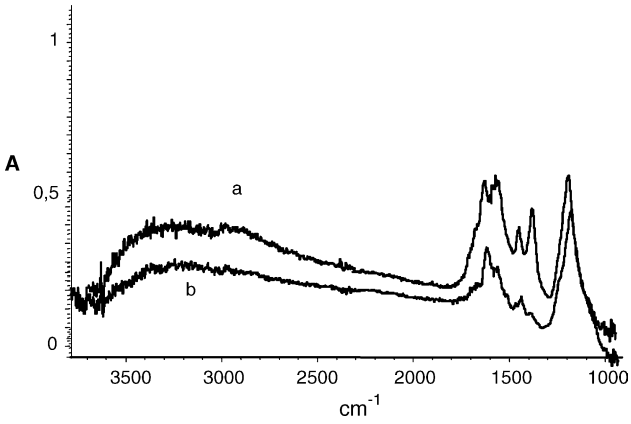

Fig. 7. FT-IR subtraction spectrum of adsorbed species arising from ammonia over a model MnO_x/TiO_2 catalyst after outgassing at RT (a) and at 423 K (b).

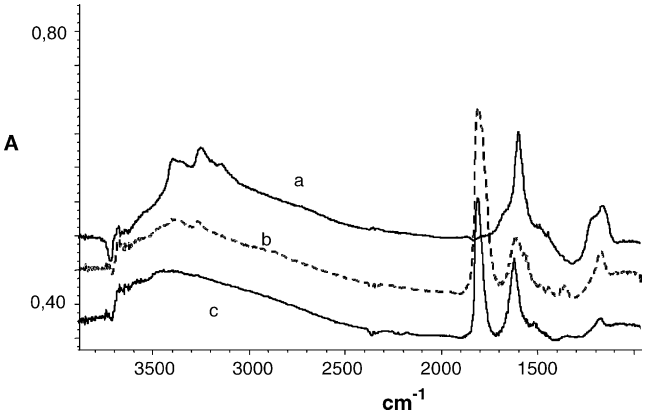

Fig. 8. FT-IR subtraction spectra of adsorbed species arising from ammonia over a model FeO_x-TiO_2 catalyst: after ammonia adsorption (a), further NO adsorption (b) and heating in NO at 523 K (c).

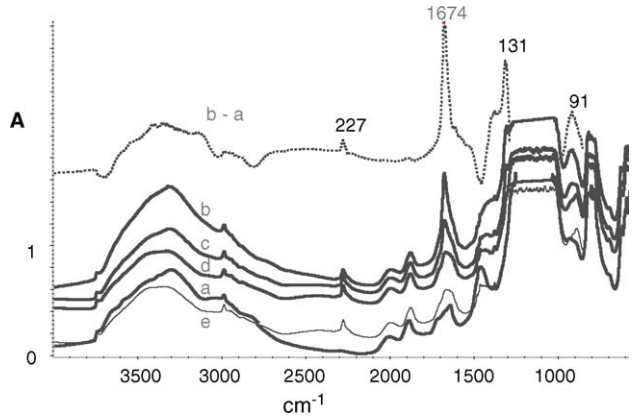

Fig. 9. FT-IR spectra of species adsorbed on HZSM5 zeolite saturated with adsorbed ammonia and outgassed at 373 K (a), and later put into contact with NO_2 at room temperature (b) and after outgassed at 323 K (c), at 348 K (d) and at 373 K (e). (b–a) Subtraction spectrum b − spectrum a.

No ammonium ions are formed in such a case, according to the total absence of protonic acidity on this catalyst. However, the surface is very active in converting ammonia in dehydrogenation and oxidized species responsible for strong bands at 1550, 1417 and 1350 cm^{-1}. These species are highly labile and disappear after outgassing even at RT. Coordinated ammonia (responsible for asymmetric and symmetric NH_3 deformation modes at 1598 and 1160 cm^{-1}) is at the origin of both dehydrogenation and oxidation, as well as of SCR of NO also in this case.

In Fig. 8, the spectra of the adsorbed species upon the SCR reaction simulated in the IR cells are reported for a Fe-TiO_2 catalyst. Also in this case no Brønsted acidity is observed at all. Ammonia is only adsorbed as coordinated species (νNH's 3400, 3252, 3144 cm^{-1}, $\delta_{as}NH_3$ 1600 cm^{-1}, $\delta_{syn}NH_3$ 1163 cm^{-1}, with a component at 1215 cm^{-1}). NO adsorbs over the ammonia-covered catalyst-giving rise to a surface nitrosyl species (νNO at 1810 cm^{-1}). By heating, the above cited bands due to coordinated ammonia decrease in intensity up to disappear while progressively bands due to adsorbed water grow at 1625 cm^{-1} and in the region near 3500 cm^{-1} (bending and stretchings, respectively) showing that, also in this case, coordinated NH_3 reacts with NO. Interestingly, the lower intensity components of the symmetric deformation band, at 1215 cm^{-1} seems to be fully eroded, while the lower frequency one converts more slowly. The two ammonia species show different reactivity.

3.2.3. Low-temperature NH_3-SCR over protonic zeolites

A different approach consists in the low-temperature NH_3-SCR over H-ZSM5 and other protonic zeolites. NO_x reduction by ammonia is observed on H-ZSM5 to occur fast at temperatures of the order of 300–473 K. In this case, however, the reaction is different, NO_2 being likely the actual reagent. It has been established that the oxidation of NO to NO_2 represents the rate-determining step in this case [23–25]. The reaction mechanism is still under discussion. The protonic center of zeolite might represent the active site where ammonia adsorbs, although the possibility of a role of extra framework material where Lewis sites are observed cannot be excluded up to now.

The spectra reported in Fig. 9 refer to the adsorption of a NO_2 rich NO_x mixture on NHU-ZSM5. NO was admixed with oxygen and left to react for several tens of minutes. The IR spectrum of the gas shows the formation of NO_2 as the predominant species in the gas, in these conditions. The spectrum recorded after contact of the pre-activated sample (Fig. 9a) with the gas is shown in Fig. 9b. The subtraction spectrum is also reported in Fig. 9b–a. The situation here is very different with respect to those of the preceding experiments. In fact, the bands associated to ammonium ions at 2960, 2800 and 1460 cm^{-1} evidently strongly decrease in intensity up to almost disappear, and are well evident as negative peaks in the subtraction spectrum as a result of contact with NO_2 at RT. In parallel, also new absorptions grow: in particular two sharp and strong bands appear at 1674 and 1312 cm^{-1}, that later decrease by successive outgassing at 323–373 K. In the meantime absorptions grow near 2900 and 2350 cm^{-1}, with a minimum in between. An additional weak band is also found after contact with NO_2 at 2278 cm^{-1}, and can be assigned to adsorbed N_2O [26].

The two sharp bands at 1674 and 1312 cm^{-1} are compatible with the asymmetric and symmetric stretching of a bent O═N–O structure, like NO_2 itself or a monodentate nitrate ion, or even of any covalently bonded ''nitro'' group. The absorptions growing near 2900 and 2350 cm^{-1}, with a minimum in between, look similar to those are due to the so-called ABC structure, which is associated to strong hydrogen bonding. However, it is not clear what molecule is H-bonded with the zeolite OH's in these conditions, taking into account that these features seem to grow when the bands at 1674 and 1312 cm^{-1} decrease in intensity.

The data presented above [27] show a very complex chemistry that cannot completely be clarified on these bases only. However, one datum is extremely evident and clear: ammonium ions react at room temperature with NO_2.

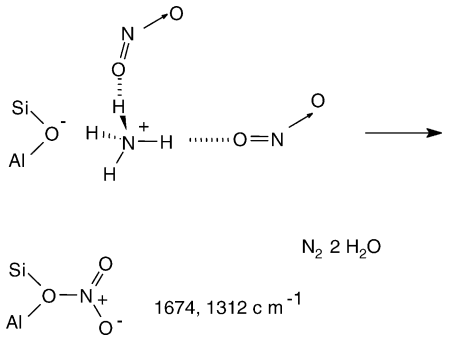

Scheme 2. First step of the reaction of NO_2 with ammonium ions over HZSM5 zeolite.

This agrees with the previous literature on the subject [23–25]. Ammonia is chemically transformed, giving rise, very probably, to N_2 and/or N_2O.

The other data reported above allow us to propose, on speculative basis, several other aspects of this chemistry. Although the identification of such species is not straightforward, the sharp and quite strong bands at 1674 and 1312 cm^{-1} may be assigned to the asymmetric and symmetric stretching of a bent O=N–O structure, like for a ''monodentate'' nitrate group which corresponds to a bent NO_2^+. The overall data we observed here suggest us that the formation of such species together with the disappearance of the bands of ammonium ions can be due to the following reported in Scheme 2.

The species responsible for the bands at 1674 and 1312 cm^{-1} can further react with residual ammonium ions to give N_2O as in the following Scheme 3.

The sequence of these two steps agrees with the stoichiometry observed for the reaction between ammonia and NO_2:

$$2NH_3 + 2NO_2 \rightarrow N_2 + N_2O + 3H_2O \quad (15)$$

In the presence of NO, instead, the redox reaction between adsorbed NO_2 and ammonium ions is apparently easier producing mostly N_2 instead of N_2O, as in the following Scheme 4. This reaction also frees the surface hydroxy groups of the zeolite.

The above reactions Schemes 1 and 3 agree with the overall stoichiometry reported in the literature for the reaction with NO + NO_2 feed:

$$2NH_3 + NO + NO_2 \rightarrow 2N_2 + 3H_2O \quad (16)$$

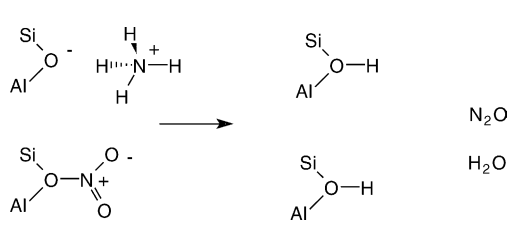

Scheme 3. Second step of the reaction of NO_2 with ammonium ions over HZSM5.

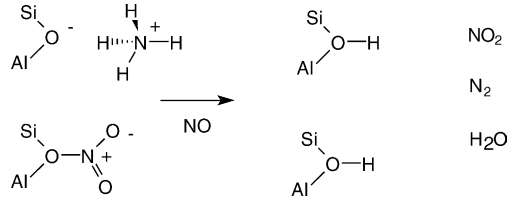

Scheme 4. Reaction between adsorbed NO_2 and ammonia in the presence of NO over HZSM5.

3.3. The CH_4-SCR reaction

The possibility for reducing NO with hydrocarbons such as olefins and higher alkanes was first proposed in 1990 by Held et al. [28] and by Iwamoto et al. [29] and Cu-MFI catalysts were found to be particularly active. However, these catalysts are poorly effective with methane as reductant. Methane as a reductant, is, however, the prefered choice for NO_x removal from flue gases of power stations because it is already present at least in methane-fueled plants. Co-containing zeolites, such as Co-MFI and Co-FER, were found by Armor [30] to be particularly active in CH_4-SCR in presence of oxygen. These catalysts work in the temperature range from 573 to 773 K and at space velocities that allow application in high-dust configurations, so being in principle a candidate to substitute ammonia-SCR.

Co^{2+} ions exchanged in a zeolitic matrix are considered to be the active sites [31], while those located at the external surface are likely inactive or can have a negative effect [32]. Catalytic activity is significantly inhibited by steam but this effect can be limited, for instance, by mixing the zeolite catalysts with metal oxides, such as manganese oxide [33].

The main drawback of these catalysts is their hydrothermal instability due to dealumination and loss of the active phase. Moreover, these catalysts are SO_x sensitive, although that effect can also be limited by modifying the zeolite composition. To improve such catalysts stability, addition of other components to Co-zeolites has been attempted. In spite of many efforts, the durability problems of transition-metal containing zeolites have not yet been resolved.

The reaction mechanism for these catalysts was also investigated [34,35]. The chemistry of NO and NO_2 with respect to Co-zeolites is very complex, and seem to significantly differ from zeolites which are very active for CH_4-SCR in presence of oxygen, like Co-Fer and Co-MFI, and those are less but still active like Co-Y. In Fig. 10, the IR spectra of the surface species formed on Co-Y after contact with NO and NO + O_2 are reported. The doublet of sharp bands formed first at 1899 and 1817 cm^{-1} have been attributed to Co^{2+} dinitrosyl species, while the broader band growing with increasing contact time at 1886, 1591 and 1300 cm^{-1} have been assigned to adsorbed N_2O_3. The couple of bands formed very strong after contact of NO + O_2 mixtures at 1489 and 1473 cm^{-1} has been assigned to symmetric nitrate species, while bands at 1632 and

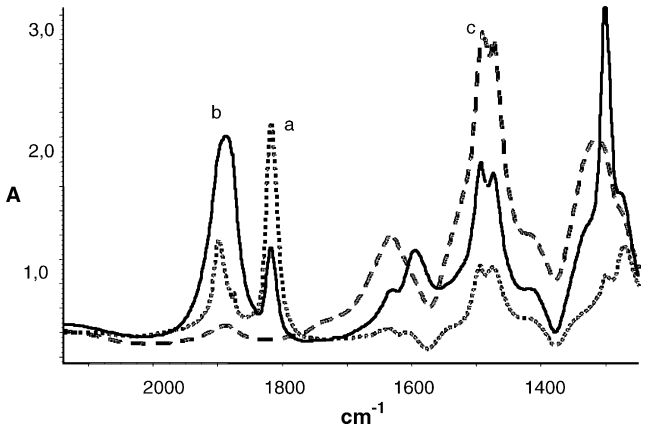

Fig. 10. Subtraction IR spectra of the surface species arising from NO adsorption on Co-Y zeolite after few minutes (a) and 1 h (b) at RT, and after contact of Co-Y to 1:1 NO:O_2 for 10 min at 473 K (c). The spectrum of the activated catalyst has been subtracted.

1317 cm^{-1} are assigned to bidentate nitrates. Such nitrate species are quite stably hald on the surface and are likely intermediates in the CH_4-SCR reaction over Co-Y. In any case most authors agree that adsorbed oxidized NO species react with methane to give N_2 [36].

According to some authors, the oxidation of NO to NO_2 can occur over protonic sites and can favor the SCR reaction. According to our recent work, however, the oxidation of NO to gaseous NO_2 could not be useful because gaseous NO_2 could not be a reaction intermediate [37]. On the other hand, this reaction occurs perhaps mainly on Co species located at the external zeolite surface, while the active intermediate is certainly associated to internal Co species. NO adsorption and its evolution to an adsorbed oxidized species are very likely. Methane reduces this intermediate adsorbate to N_2, via a complex mechanism.

3.4. Comparison with other denoxing technologies

3.4.1. The three way catalysts

The actual catalytic converters are constituted by Pt–Pd–Rh binary or ternary alloys deposited over CeO_2–ZrO_2–Al_2O_3 washcoats deposited on cordierite honeycombs [38,39]. The addition of Ceria compounds to alumina washcoats gives the oxygen-storage effect to buffer the lean-rich swings in exhaust gas composition. The active metal component is reported to be rhodium, platinum and palladium having the main role of stabilizing Rh in a reduced state. Over the Pt–Rh alloy NO is dissociatively adsorbed while CO is oxidized to CO_2 by adsorbed oxygen atoms.

3.4.2. NO_x storage-reduction (NSR) processes

NO_x storage-reduction systems represent a valuable solution for engines, which operate alternately under lean and rich conditions. NO_x are stored on oxide basic materials like Ba-alumina or alkali oxide doped alumina. These materials contain noble metal like Pt, to favor both NO oxidation upon storage and the reduction step. Various oxidized species like monodentate and bidentate nitrites, nitrates and NO_2^+ species are observed in the storage step, which are stable up to 750–900 K. Bulk barium nitrate is also observed to replace Ba carbonate present in the fresh catalyst. The reduction of such stored species occurs via a complex mechanism.

3.4.3. N_2O catalytic decomposition

The catalytic decomposition of N_2O can be obtained on different transition metal or noble metal-containing systems. However, reaction temperatures not lower than 573 K are needed to obtain significant abatement of the compound [12]. The addition of a reductant does not seem to improve very much the catalytic activity. Spectroscopic studies allowed to reveal the end-on adsorption of N_2O through its N-end and through its O-end, as well as species identified as N_2O^-, which are most likely the intermediates in the catalytic decomposition.

3.4.4. NO catalytic decomposition

The only well-known system that has significant activity in the decomposition of NO to N_2 and O_2 is that of Cu-zeolites [11]. The zeolites can be prepared by ion exchange and by gas phase deposition procedures. Multiple ion exchange procedures are usually performed with Cu^{2+} salts and the resulting material can be over-exchanged (Cu^{2+}/Al^{3+} atomic ratios >0.5) possibly because of the autoreduction of Cu^{2+} to Cu^+. Over-exchanged catalysts are the most active. Most authors believe that extralattice oxygen also exists in over-exchanged catalysts although some controversy exists on the possible role of dimeric Cu–O–Cu complexes or in monomeric Cu–O species. Although it seems sure that NO decompostion is a redox reaction, occurring though Cu^+/Cu^{2+} cycles, the details of the reaction mechanism are still under discussion.

4. Conclusions

On the basis of the data discussed above, a comprehensive view of the chemistry of NO_x upon processes for DeNOxing can be attempted. In particular, we can find processes and catalysts where NO_x are ‘‘activated’’. This is the case, e.g. of the zeolite catalysts for CH_4-SCR as well as over the adsorbents/catalysts over which the storage and reduction occurs, where they are activated by oxidation to a very active adsorbed form. It seems likely that the formation of gas phase NO_2 is not a necessary step. On the contrary, over the noble metal catalysts where reduction by CO occurs, NO is activated by dissociation. Probably, something similar occurs over Cu-zeolite catalysts for NO decomposition: in both cases NO oxidizes the catalyst by reducing itself.

Just the opposite occurs over the catalysts for NH_3-SCR: in this case the reductant (ammonia) is activated in form of coordinated species over reducible cations (V^{5+}, Mn^{4+},

Fe^{3+}). In the case of low-temperature NH_3-SCR over protonic zeolites, both ammonia and NO, have to be activated. NO is certainly activated by oxidation to NO_2, while NH_3 is activated on acid sites (either Brønsted sites or Lewis sites). It seems likely that the protonation of ammonia is too weak as activation and needs for reaction of a highly oxidant species like NO_2. On the contrary, the coordination over high oxidation state cations gives rise to a highly reactive complex allowing reaction with NO.

References

[1] A.R. Butler, R. Nicholson, Life, Death and Nitric Oxide, RSC, Cambridge, 2003.
[2] V.I. Pârvulescu, P. Grange, B. Delmon, Catal. Today 46 (1998) 233.
[3] J. Kaspar, P. Fornasiero, N. Hickey, Catal. Today 77 (2003) 419.
[4] G. Busca, F. Bregani, G. Rocchini, Inquinamento 34 (2002) 40.
[5] R.C. Reid, J.M. Prausnitz, B.E. Poling, The Properties of Gases and Liquids, fourth ed., McGraw Hill, New York, 1987.
[6] G. Olofsson, W. Wang, Z. Ye, I. Bjerle, A. Andersson, Energy Fuels 16 (2002) 915.
[7] S. Naha, S.K. Aggarwal, Combust. Flame 139 (2004) 90.
[8] Environmental Processes, Hydrocarbon Processing, Gulf Publication, August 1998.
[9] F. Kohler, H.J.R. Guedes, J.C. Revés, M. Nunes das Ponte, J. Mol. Liquids 67 (1995) 105.
[10] I.C. Hisatsune, J. Phys. Chem. 65 (1961) 2249.
[11] H. Yahiro, M. Iwamoto, Appl. Catal. A: Gen. 222 (2001) 163.
[12] J. Pérez-Ramìrez, F. Kapteijn, K. Schoffel, J.A. Moulijn, Appl. Catal. B: Environ. 44 (2003) 117.
[13] S. Alini, A. Bologna, F. Basile, T. Montanari, A. Vaccari, European Patent l,83035°l (2001).
[14] G. Busca, J. Raman Spectrosc. 33 (2002) 348.
[15] L.J. Alemany, F. Berti, G. Busca, G. Ramis, D. Robba, G.P. Toledo, M. Trombetta, Appl. Catal. B: Environ. 10 (1996) 299.
[16] G. Busca, L. Lietti, G. Ramis, F. Berti, Appl. Catal. B: Environ. 18 (1998) 1.
[17] H. Bosch, F. Janssen, Catal. Today 2 (1988) 369.
[18] M. Anstrom, N.Y. Topsøe, J.A. Dumesic, J. Catal. 213 (2003) 115.
[19] K. Jug, T. Homann, T. Bredow, J. Phys. Chem. A 108 (2004) 2966.
[20] M. Koebel, G. Madia, F. Raimondi, A. Wokaun, J. Catal. 209 (2002) 159.
[21] G. Ramis, G. Busca, F. Bregani, P. Forzatti, Appl. Catal. 64 (1990) 259.
[22] L. Lietti, G. Ramis, F. Berti, P. Toledo, D. Robba, G. Busca, P. Forzatti, Catal. Today 42 (1998) 101.
[23] M. Richter, R. Eckelt, B. Parlitz, R. Fricke, Appl. Catal. B: Environ. 15 (1998) 129.
[24] S.A. Stevenson, J.C. Vartuli, J. Catal. 208 (2002) 100.
[25] M. Wallin, C.J. Karlsson, M. Skoglundh, A. Palmqvist, J. Catal. 218 (2003) 354.
[26] G. Ramis, G. Busca, F. Bregani, Gazzetta Chim. Ital. 122 (1992) 79.
[27] V. Sanchez Escribano, T. Montanari, G. Busca, Appl. Catal. B: Environ. 58 (2005) 19.
[28] W. Held, A. Konig, T. Richter, L, Puppe, Soc. Aut. Eng. Paper 900496, 1990.
[29] M. Iwamoto, H. Yahiro, Y. Shundo, Y. Yu-u, N. Mizuno, Shokubai 32 (1990) 430.
[30] J.N. Armor, Catal. Today 26 (1995) 147.
[31] T. Montanari, M. Bevilacqua, C. Resini, G. Busca, J. Phys. Chem. B 108 (2004) 2120.
[32] G. Bagnasco, M. Turco, C. Resini, T. Montanari, M. Bevilacqua, G. Busca, J. Catal. 225 (2004) 536.
[33] M. Misono, Cattech 2 (1998) 183.
[34] A.J. Desai, V.I. Kovalchuk, E.A. Lombardo, J.L. D'Itri, J. Catal. 184 (1999) 396.
[35] S.A. Beloshapkin, E.A. Paushktis, V.A. Sadykov, J. Mol. Catal. A: Chem. 158 (2000) 355.
[36] K. Hadjiivanov, D. Klissurski, G. Ramis, G. Busca, Appl. Catal. B: Environ. 7 (1996) 251.
[37] C. Resini, T. Montanari, L. Nappi, G. Bagnasco, M. Turco, G. Busca, F. Bregani, M. Notaro, G. Rocchini, J. Catal. 214 (2003) 179.
[38] M. Shelef, R.W. McCabe, Catal. Today 62 (2000) 35.
[39] J. Kaspar, P. Fomasiero, N. Hickey, Catal. Today 77 (2003) 419.